arXiv:2412.04378v2 [cs.CV] 8 Dec 2024

Discriminative Fine-tuning of LVLMs

Yassine Ouali*[1] Adrian Bulat*[1,2] Alexandros Xenos[1,3] Anestis Zaganidis[1]
Ioannis Maniadis Metaxas[1] Brais Martinez[1] Georgios Tzimiropoulos[1,3]
[1]Samsung AI Cambridge [2]Technical University of Iasi [3]Queen Mary University of London

Abstract

Contrastively-trained Vision-Language Models (VLMs) like CLIP have become the de facto approach for discriminative vision-language representation learning. However, these models have limited language understanding, often exhibiting a "bag of words" behavior. At the same time, Large Vision-Language Models (LVLMs), which combine vision encoders with LLMs, have been shown capable of detailed vision-language reasoning, yet their autoregressive nature renders them less suitable for discriminative tasks.

In this work, we propose to combine "the best of both worlds": a new training approach for discriminative fine-tuning of LVLMs that results in strong discriminative and compositional capabilities. Essentially, our approach converts a generative LVLM into a discriminative one, unlocking its capability for powerful image-text discrimination combined with enhanced language understanding.

Our contributions include (1) A carefully designed training/optimization framework that utilizes image-text pairs of variable length and granularity for training the model with both contrastive and next-token prediction losses. This is accompanied by ablation studies that justify the necessity of our framework's components. (2) A parameter-efficient adaptation method using a combination of soft prompting and LoRA adapters. (3) Significant improvements over state-of-the-art CLIP-like models of similar size, including standard image-text retrieval benchmarks and notable gains in compositionality.

1. Introduction

Contrastively-trained Vision Language Models (VLMs) (e.g. CLIP [36]) have become the predominant direction for vision-language representation learning, exhibiting remarkable zero-shot abilities [21, 28, 31, 36, 48]. However, the great success of these models in many vision-language and vision tasks, even in a zero-shot manner, "sweeps under the rug" some of their important limitations. Specifically, such models struggle to exhibit advanced language understanding capabilities, suffer from a limited understanding of compositionality, and manifest a *bag of words* behavior [25, 47]. For example, even with *bag of words* behavior, VLMs have shown remarkable zero-shot retrieval accuracy on the Flickr [46] and COCO [33] datasets. Still, they perform poorly on a simple word order permutation task on the same datasets [47]. Unfortunately, these issues persist even when the model and the dataset size increase [19].

Concomitantly, inspired by the success of LLMs [5, 42] in acting as generalist assistants [15], a series of works combine pretrained vision encoders and LLMs [26, 27, 50] to construct Large Vision-Language Models (LVLMs) capable of performing interactive multi-modal conversations between the model and the user. Among others, these models have been shown capable of *exhibiting strong reasoning and vision-language understanding capabilities*, offering fine-grained and detailed responses [9, 11, 26, 27]. However, they are trained with a next-token prediction loss in an autoregressive manner, which appears less suitable for direct utilization in discriminative image-text tasks (*e.g.* image-text retrieval).

To our knowledge, the very recent (concurrent) work [23] is the first one to show that, with appropriate prompting, LVLMs can serve as zero-shot discriminative models. Importantly, [23] advocates for a text-text optimization approach, stating that contrastive image-text fine-tuning has a detrimental effect on the model's performance. In contrast to [23], we propose a new training framework for discriminative image-text fine-tuning of LVLMs, aiming to convert the original *generative* LVLM into a *discriminative* one, thereby significantly enhancing its capability for image-text discrimination while preserving the compositional strengths of the original model.

In our approach, following the (independent) two-towers paradigm, the vision embeddings are produced by passing the image through the entire LVLM, and the text embeddings are produced by passing the text through the LLM of the LVLM. Intuitively, for vision embedding, the LLM acts as an information extractor/processor that refines the visual information extracted by the data while simultane-

* Equal contribution. Listing order is random.

ously aligning the visual representations with the textual ones. We coin our approach **VladVA**: **V**ision-**L**anguage **A**daptation for **D**iscriminative **V**isual **A**ssistant.

Our **main contributions** are:

- We devise a carefully designed optimization framework that utilizes image-text pairs of variable length and granularity for model training (*i.e*. both short and long captions). Using this data, the model is trained with both contrastive and next-token prediction losses, which are both shown to be necessary for unlocking strong discrimination and compositionality capabilities. Our design choices are accompanied by ablation studies which justify the necessity of our framework's components.
- To facilitate efficient training, we show how the model can be fine-tuned using a parameter-efficient adaptation method based on a combination of soft prompting [30] and LoRA adapters [20]. We show the positive impact of both components.
- We report significant improvements over state-of-the-art two-tower models (e.g. CLIP-like models) of similar size on standard image-text retrieval benchmarks (+4.7-7.0% gains in absolute terms). Moreover, we report notable gains on several vision-language understanding and compositionality benchmarks (up to +15%).

2. Related work

2.1. Large Vision Language Models (LVLMs)

Inspired by breakthrough research in language modeling [5, 22, 40, 42], a series of methods seek to combine pretrained LLMs and vision encoders to construct Large Vision Language Models (LVLMs) capable of processing image-text data jointly [3, 11, 32, 34, 35, 44, 45, 50]. The prevalent strategy consists in aligning the features produced by a pretrained vision encoder to the textual space assumed by a pretrained LLM using a projection module, *e.g*. LLaVA [35], following a two-stage alignment procedure. Follow-up works expand this to interleaved image-text data [1, 27] and multiple input crops [1] while seeking to improve the model's efficiency [10].

Despite their strong generative and comprehension abilities [34], current LVLMs are primarily restricted to generative tasks. Only very recently, Jiang *et al*. [23], inspired by the recent progress in NLP [4, 24] adapted a LLaVA-NeXT [26] model to discriminative tasks with the help of a contrastive-like loss, using text data only. We note that unlike [23], we introduce a training framework that learns from multi-turn image-text pairs (as opposed to text only) using a novel formulation that jointly combines a contrastive loss with a next-token prediction, reflecting the data characteristics and inducing a gradual representation buildup. Moreover, we compare our approach with E5-V [23], significantly improving upon their results despite using smaller/lighter models.

2.2. Discriminative Vision-Language Models

The prevalent approach for training Discriminative VLMs follows the two-tower contrastive approach pioneered by CLIP [36], whereby an image and text encoder are trained on web-collected image-text pairs to learn a joint multi-modal (i.e., vision and language) space. Subsequent works build upon CLIP by scaling the data [37, 48], improving the architecture using late/early interactions [29] or improving the training loss [7, 48]. Despite their remarkable zero-shot and representation learning abilities [36] such models were shown to have significant shortcomings related to limited language understanding capabilities, including: lack of compositionality understanding [25], manifesting *bag of words* behavior [47], struggling with spatial relations [25], being susceptible to typographical attacks [17], *etc*. Recent works aim to address these shortcomings by constructing synthetic hard negatives [47] or performing cross-modality attention [29]. However, the former does not inherently change the model's behaviors and has been shown to potentially learn a series of shortcuts/artifacts [19]. Meanwhile, the latter is impractical for deployment at scale, as, due to the interactions between the encoders, each new query incurs an additional inference for every image within the set.

To alleviate these shortcomings and improve the overall capabilities of such models, we depart from the prevalent approach of training VLMs using a contrastive loss and, instead, propose a new approach that seeks to convert generative LVLMs into discriminative models by adapting them using a newly proposed framework that combines generative and discriminative objectives.

3. Method

The following sections detail our approach which we call **VladVA**: **V**ision-**L**anguage **A**daptation for **D**iscriminative **V**isual **A**ssistant.

3.1. LVLMs as zero-shot discriminative models

LVLMs consist of an LLM Φ_t, a vision encoder Φ_v, and a module g that projects the vision features into the LLM's textual space. Once fine-tuned, such models can produce a textual answer $\mathbf{x}_a = \Phi_t(g(\Phi_v(\mathbf{x_v})), \mathbf{x}_q)$ when presented with an input image $\mathbf{x}_v$ and a text query (or prompt) $\mathbf{x}_q$.

Despite being solely trained with an autoregressive next-token prediction loss on limited amounts of data ($<$ 5M), such models can act as multi-modal discriminative models in a zero-shot manner [23]. To elicit this capability, the image embedding $\mathbf{f}_v = \Phi_t(g(\Phi_v(\mathbf{x_v}), \mathbf{x}_p)[eos]$ is obtained by passing the image alongside a handcrafted prompt $\mathbf{x}_p$ through the LVLM and taking the last token, prior to any generation, as the reference feature. Analogously, the text

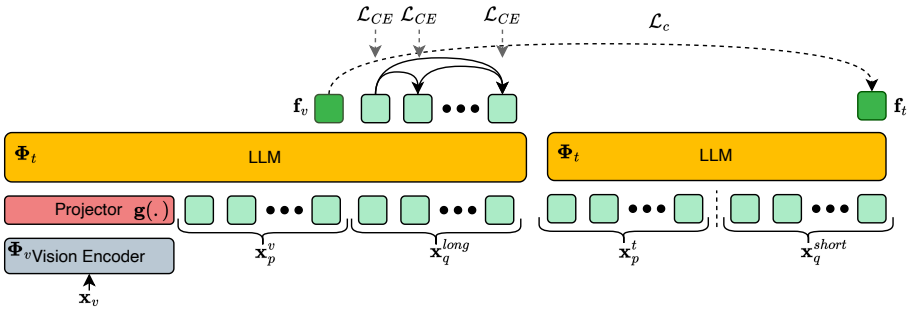

Figure 1. **Overall VladVA framework:** a generative LVLM is adapted into a discriminative model. At test time, the vision features ($\mathbf{f}_v$) are produced by passing the image $\mathbf{x}_v$ alongside the handcrafted and/or soft prompt $\mathbf{x}_p^v$ to the LVLM. The last token of this sequence will contain the summarized representation. Analogously, the textual features ($\mathbf{f}_t$) are produced by passing the prompt corresponding to the language modality ($\mathbf{x}_p^t$) through the LLM of the LVLM (*i.e.* the weights of the LLM are fully shared) alongside the short caption ($\mathbf{x}_q^{short}$). During training, the LVLM will also take as input a long, detailed caption $\mathbf{x}_\mathbf{q}^\mathbf{long}$.

embedding $\mathbf{f}_t = \Phi_t(\mathbf{x}_p, \mathbf{x}_q)[eos]$ is produced by passing the handcrafted prompt $\mathbf{x}_p$ and input $\mathbf{x}_q$ query through the LLM of the LVLM and taking again the features of the last token, prior to any autoregressive step. We will refer to these particular tokens as "summary tokens". Note that, typically, the respective handcrafted prompts for the image and text modalities are different. Finally, the similarity between an image and a given text can be computed by taking the cosine similarity between the two: $s = \texttt{cos_sim}(\mathbf{f}_v, \mathbf{f}_t)$.

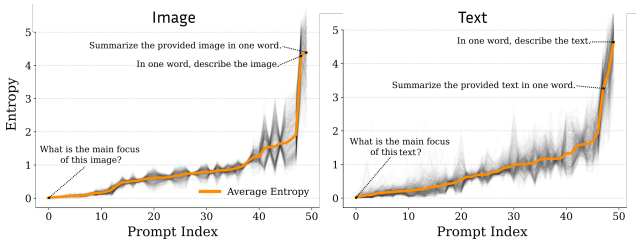

Figure 2. **Entropy of the output probability distribution** at the next-to-be-predicted token location using a LLaVA-1.5-7B for a set of 50 prompts for both images and captions.

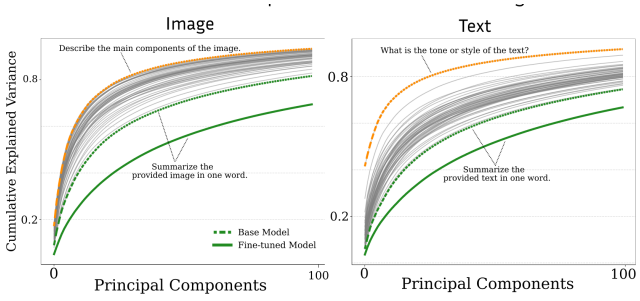

Figure 3. **Cumulative variance of the image and text embedding matrices** over a set of 50 prompts on Flickr30k. Embeddings that capture more information about the input translate into a cumulative variance that requires more principal components to be explained, *i.e.* a higher rank embedding matrix.

What makes a good prompt? Zero-shot adaptation by prompting already provides decent results despite the task changing from generation to discrimination. To shed some light, herein, we study (a) what makes a good prompt and (b) how we can identify it.

To answer these questions, we construct a testbed consisting of 1,000 image-caption pairs from Flickr30k [46], which we then use to evaluate the quality of various prompts. The prompts (50 image-text pairs in total) are constructed using ChatGPT. Each prompt pair is fed, alongside an image and its respective caption, through the LLaVA-1.5-7B model. For each image-prompt pair and, respectively, caption-prompt pair, we take its token embedding at the output position and its output probability distribution over the vocabulary and use them to compute two measures for each prompt: the average entropy of its output distributions and the cumulative variance of its embeddings. As Figs. 2 and 4 show, when the model is prompted with sentences consisting of certain keywords, such as `in a few words` or in `one word`, the model is pushed to condense the information of the image or text in the next token, resulting in an output distribution with high entropy. More importantly, when investigating the generated embeddings, we observe that higher entropy prompts result in embeddings with more spread-out cumulative variance, *i.e.* requiring more principal components to capture the same amount of variance, indicating an embedding matrix with a high rank (see Fig. 3). This translates into discriminative embeddings that can capture more information about the inputs, making them suitable for embedding tasks. The benefit of this behavior is illustrated in Fig. 5, which shows a positive correlation between prompts with high entropy scores and the model's zero-shot retrieval performance. Hence, our approach should seek to produce embeddings with a) spread-out variance and b) probability distributions over the vocabulary with increased entropy.

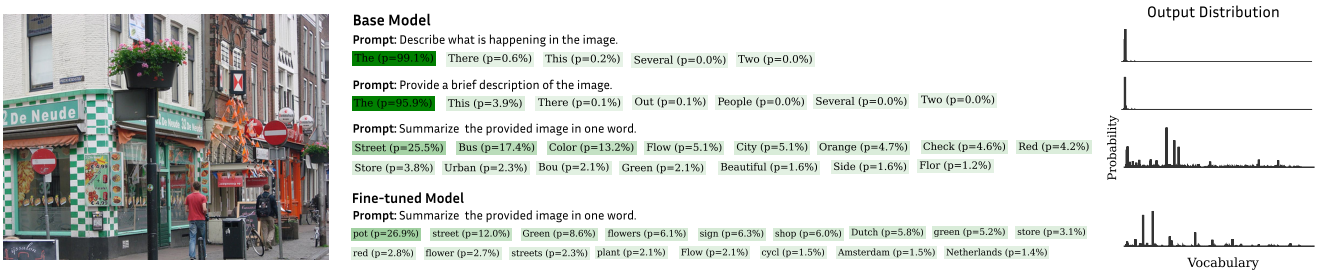

Figure 4. **Top-k next-to-be-predicted tokens** before and after the proposed fine-tuning approach. On the right, we show the output probability distribution for each case. We observe that, when using the optimal prompt, the representations of the next token can encode diverse and more discriminative information, making potentially better-quality embeddings. This behavior is further improved by the proposed fine-tuning method.

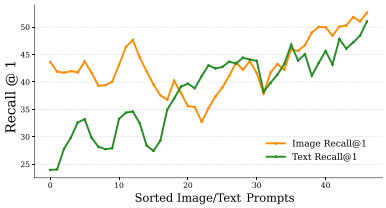

Figure 5. **Image and text retrieval score on Flickr30k** over a set of 50 image-text prompts ordered by their entropy scores (Fig. 2). We can observe that prompts with high average entropy scores correlate positively with the zero-shot retrieval performance.

3.2. Discriminative fine-tuning of LVLMs: from generation to discrimination

Despite exhibiting surprising innate zero-shot abilities, LVLM's direct discriminative performance lags behind that of state-of-the-art contrastively trained VLMs. Hence, carefully designed frameworks are needed to unlock the full potential of such models. This is the very goal of our work: to introduce a well-grounded *image-text* adaptation/training framework that surfaces the discriminative vision-language capabilities of a generative LVLM.

Notably, our findings contradict those of the very recent (concurrent) work of [23], which found that contrastive image-text fine-tuning is detrimental and limits training to text-text contrastive learning alone. This highlights the importance of our proposed approach, which overcomes such impediments and significantly boosts the discriminative performance of the model.

Having established the architecture in the previous section, the two other pillars are the data and training strategy.

Data strategy: We argue for the importance of data diversity in terms of granularity and group captions according to their length: short captions (< 30 tokens) and long captions ($30 - 500$ tokens). The short captions capture coarse details and summarize image content, which teaches the model to discriminate with regard to the high-level information of an image. Longer captions capture finer details in images and promote a better understanding of language concepts such as spatial relationships and compositionality. For a strong discriminative model, both are necessary. Therefore, for images missing either caption type, we use a BLIP2 [29] captioner to generate short captions and ShareGPT-4V [8] to generate long captions. This allows us to leverage both supervisory signals for training.

Training strategy: As we demonstrate in this work, the variable length of the training data poses its own challenges: unlike the case of short captions, where direct training using the well-studied contrastive loss performs well, it collapses for longer captions. This brings us to the proposed training strategy, whereby, to address this challenge, we propose a well-motivated hybrid training approach that combines a contrastive loss (see Sec. 3.2.1) and a *next-token prediction loss for discriminative adaptation* (see Sec. 3.2.2). Finally, as full model fine-tuning is computationally expensive, in Sec. 3.3, we detail a fine-tuning strategy that combines adapters with soft prompting.

3.2.1. Image-text contrastive alignment

Under a multi-modal contrastive formulation, the image and text representations, $\mathbf{f}_v$ and $\mathbf{f}_t$ respectively, must be close if they are semantically similar and far apart otherwise, under a specified distance metric. At train time, this is enforced using a symmetric image-text and text-image contrastive loss, which, for a given mini-batch containing b randomly selected samples, can be described as:

$$\mathcal{L}_c = \frac{1}{b}\sum_{k=1}^{b}\left(-\log\frac{\exp(s_v^{k,k})}{\sum_j \exp(s_v^{k,j})} - \log\frac{\exp(s_t^{k,k})}{\sum_j \exp(s_t^{j,k})}\right), \tag{1}$$

where $s_v^{k,j} = \texttt{cos_sim}(\mathbf{f}_v^k, \mathbf{f}_t^j)$ denotes the cosine similarity between the k-th image and the j-th caption (image-to-text), and similarity, $s_t^{k,j}$ the text-to-image similarity.

During training, the contrastive loss is applied to the very same tokens used for the zero-shot evaluation, as they represent the optimal starting point for further fine-tuning. We note that the contrastive loss is mostly suitable for train-

ing using short captions (< 30 tokens), like the ones typically used for CLIP pre-training. We found that training the model using a contrastive loss on longer captions proves challenging. Hence, to address this, in the following section, we study and propose a new formulation that enables discriminative training on variable-length data.

3.2.2. Autoregressive training for learning discriminative LVLM representations

Until now, the modality-specific embeddings are obtained by taking the last token, prior to any generation, while the training is largely focused on short (*i.e.* < 30 tokens) captions, mimicking the CLIP-style data used for contrastive training. This contrasts with the LLaVA-style autoregressive training, where long and highly descriptive captions (typically 200–500 tokens) are used to help the LVLM learn strong links between the vision and text domains, pay attention to fine-grained details, and develop strong reasoning and compositionality capabilities.

As noted earlier, directly using the long captions with the contrastive loss is ineffective, as, due to the high specificity of the long captions, the task is easy and nearly trivial to solve, with the loss going to 0 in just a few hundred iterations. To address this, we propose to instead apply the next-token prediction loss over the long captions:

$$\mathcal{L}_{CE} = \sum_{i=1}^{L} \log p_\theta(u_i | \mathbf{x}_v, \mathbf{x}_p, \mathbf{x}_{q,<i}), \tag{2}$$

where L is the length of the long caption, $\mathbf{x}_q$, $\mathbf{x}_v$ the input image and $\mathbf{x}_p$ the prompt, and p_θ as the next-token probability distribution produced by the model at input token u_i.

Intuitively, this formulation possesses multiple advantages: (1) It allows the model to learn from long captions, as predicting each and every token correctly is a challenging task (as opposed to applying the contrastive loss to long captions). (2) The decoding process encourages the condensation of information into the starting token used as a feature embedding. (3) It offers an avenue for retaining the generative capabilities of the model while strengthening its discriminative abilities.

3.2.3. Overall training loss

We apply the next-token prediction loss over the long captions and the contrastive loss over the short ones in a unified manner. During training, the templates presented to the LVLM for the image and, respectively, text modality take the following form:

Template for the image modality:
`USER: [Image Prompt] <image>`
`ASSISTANT: <out_token>`
`USER: Describe the image in detail.`
`ASSISTANT: <long_caption> <out_token>`
Template for the text modality:
`USER: [Text Prompt] <short_caption>`
`ASSISTANT: <out_token>`

with the contrastive loss applied between the `<out_token>` belonging to the image modality on one side, and the text modality on the other. Concomitantly, the next-token prediction cross-entropy loss is applied over the tokens belonging to the `<long_caption>`. Note that the short caption must be sufficiently different from the long caption to prevent shortcuts during training, a property that does not naturally emerge in our case due to the difference in length and annotation procedure.

3.3. Parameter Efficient Adaptation

As direct fine-tuning of the LVLM is costly, especially while attempting to maintain a reasonably large batch size for contrastive learning, herein we explore and adopt soft-prompting combined with LoRA adapters, both trained under the same loss formulation of Sec. 3.2.

Soft prompting was recently proposed as an efficient task-adaptation approach for both LLM [30] and CLIP [6, 49] models, representing a direct departure from the prompt hand-crafting solution. Specifically, for a given input modality, *i.e.* image and text, we define a set of n modality(m)-specific learnable vectors $[\mathbf{v}_1^m, \mathbf{v}_2^m, \cdots, \mathbf{v}_n^m]$, $\mathbf{v}_i^m \in \mathbb{R}^C$ with C denoting the model's vocabulary embedding size. These vectors can be inserted across the input sequence to adjust the model's behavior. In practice, we opt to replace the tokens belonging to the hard prompts (*i.e.* $\mathbf{x}_p$; see Sec. 3.1) with the learnable vectors, initializing their values with the embeddings of the handcrafted ones.

Adapter fine-tuning: While efficient, the representation power of the soft prompts is somewhat limited. Hence, following best practices, we also attach LoRA [20] adapters to the linear layers located inside Φ_t. Such adapters offer a multifold advantage: lower memory requirements, reduced potential of overfitting during training, and no additional compute requirements during inference.

The model is fine-tuned using these components. Importantly, both have a positive impact on overall accuracy.

3.4. How does the model's behavior change?

Building upon the analysis from Sec. 3.1, we show that our training approach elicits the following *behavioral* changes: (1) The summary token - vision tokens' attention increases in density. (2) Both the entropy of the output distribution of the summary token and the spread of the cumulative vari-

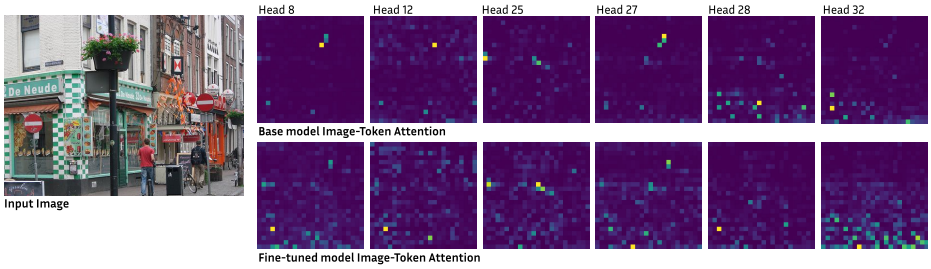

Figure 6. **Attention map between the summary and vision tokens shown for a set of heads**. Notice that post-training, the attention maps densify. This behavioral change can be interpreted as follows: For generative tasks, at every step in the generation process, the model has the chance to look back at the vision tokens, selectively attending to the regions of interest at the current step. In contrast, in a discriminative setting, the model must compress all information present in the image within the summary token.

Table 1. Zero-shot text-image retrieval accuracy on Flickr30K, COCO and nocaps.

Method	**image** retrieval						**text** retrieval					
	Flickr30K		COCO		nocaps		Flickr30K		COCO		nocaps	
	R@1	R@10	R@1	R@10	R@1	R@10	R@1	R@10	R@1	R@10	R@1	R@10
CLIP (`ViT-B`) [36]	58.8	89.8	30.5	66.8	46.8	85.1	77.8	98.2	51.0	83.5	67.3	95.6
CLIP (`ViT-L`) [36]	67.3	93.3	37.0	71.5	48.6	85.7	87.2	99.4	58.1	87.8	70.0	96.2
BLIP (`ViT-L`) [28]	70.0	95.2	48.4	83.2	62.3	93.4	75.5	97.7	63.5	92.5	72.1	97.7
BLIP2 (`ViT-L`) [29]	74.5	97.2	50.0	86.1	63.0	93.8	86.1	99.4	63.0	93.1	74.4	98.3
OpenCLIP (`ViT-G/14`) [37]	77.8	96.9	48.8	81.5	63.7	93.2	91.5	99.6	66.3	91.8	81.0	98.7
OpenCLIP (`ViT-BigG/14`) [37]	79.5	97.1	51.3	83.0	65.1	93.5	92.9	97.1	67.3	92.6	82.3	98.8
EVA-02-CLIP (`ViT-E/14+`) [38]	78.8	96.8	51.1	82.7	64.5	92.9	93.9	99.8	68.8	92.8	83.0	98.9
EVA-CLIP (`8B`) [39]	80.3	97.2	52.0	82.9	65.3	93.2	94.5	99.7	70.1	93.1	83.5	98.6
EVA-CLIP (`18B`) [39]	83.3	97.9	55.6	85.2	69.3	94.8	**95.3**	99.8	72.8	94.2	85.6	99.2
LLaVA-1.5-7B [34]	59.6	89.3	34.4	69.6	46.9	83.3	65.6	92.3	35.6	70.5	52.1	88.1
E5-V (`LLaVA-Next-8B`) [23]	79.5	97.6	52.0	84.7	65.9	94.3	88.2	99.4	62.0	89.7	74.9	98.3
E5-V (`LLaVA-1.5-7B`) [23]	76.7	96.9	48.2	82.1	62.0	93.0	86.6	99.0	57.4	88.4	71.9	97.0
VladVA (Ours) (`LLaVA-1.5-7B`)	**85.0**	**98.5**	**59.0**	**88.6**	**72.3**	**96.5**	94.3	**99.9**	**72.9**	**94.4**	**85.7**	**99.5**

ance of the embeddings increase.

The attention map densification, as exemplified in Fig. 6, shows that, for discriminative tasks, the model gathers evidence from all parts of the image in order to correctly encode the information therein. This is not needed for generation, as at every generation step, the model can "peak back" at the vision tokens and select the required information.

Entropy and cumulative variance: As shown in Fig. 3, our approach results in models where the cumulative variance of the image and text embeddings is significantly more spread out, which translates into richer and better-aligned embeddings, capable of more accurately capturing fine-grained details. Additionally, the model maintains the diversity of output distribution at the summary token, *i.e*. high entropy, as illustrated in Fig. 4.

4. Experiments

We compare our approach with the current state-of-the-art on two tasks of interest in a zero-shot manner: image-text retrieval and compositionality/language understanding.

Models compared: We compare with state-of-the-art models based on the two-towers (independent) approach, which is practical for retrieval purposes and also followed by our method. We cover a wide variety of settings, including different models and model sizes, training data, training losses, etc.: CLIP (`ViT-B` and `ViT-L`) [36] – the original CLIP trained with a contrastive loss on 400M image-text pairs; BLIP (`ViT-L`) [28] – trained on over 120M samples using contrastive, captioning and image-text matching losses; BLIP2 (`T5-XXL`) – improved and scaled-up version of BLIP that makes use of qformer and LLM; OpenCLIP (`ViT-G/14`) [37] – scaled-up version of [36] trained on 2B samples; OpenCLIP (`ViT-BigG/14`) [37], EVA-02-CLIP (`ViT-E/14+`) [38], EVA-CLIP (`8B`) [39] and EVA-CLIP (`18B`) [39] – large contrastively trained models, with up to 18B parameters, fine-tuned from vision encoders trained with Masked Image Modeling (MIM); E5-V (`LLaVA-Next-8B`) and E5-V (`LLaVA-1.5-7B`) – LVLMs finetuned using a text-text contrastive loss. Depending on the task, we also include additional specialized baselines (*e.g*. NegCLIP [47] for compositionality).

Table 2. Comparison with state-of-the-art on the SugarCrepe compositionality benchmark.

Method	Params	Replace			Swap		Add	
	(B)	Object	Attribute	Relation	Object	Attribute	Object	Attribute
Human	–	100	99	97	99	100	99	99
CLIP (ViT-B) [36]	0.15	90.9	80.1	69.2	61.4	64.0	77.2	68.8
CLIP (ViT-L) [36]	0.43	94.1	79.2	65.2	60.2	62.3	78.3	71.5
BLIP (ViT-L) [28]	0.23	96.5	81.7	69.1	66.6	76.8	92.0	85.1
BLIP2 (ViT-L) [29]	1.17	97.6	81.7	77.8	62.1	65.5	92.4	87.4
OpenCLIP (ViT-G/14) [37]	1.37	95.8	85.0	72.4	63.0	71.2	91.5	82.1
OpenCLIP (ViT-BigG/14) [37]	2.54	96.6	87.9	74.9	62.5	75.2	92.2	84.5
EVA-02-CLIP (ViT-E/14+) [38]	5.04	97.1	88.5	74.2	67.3	74.1	91.8	83.9
EVA-CLIP (8B) [39]	8.22	96.4	86.6	74.8	66.1	74.6	91.3	82.0
EVA-CLIP ((18B) [39]	18.3	97.5	88.8	76.1	65.3	76.0	92.4	85.0
NegCLIP [47]	0.15	92.7	85.9	76.5	75.2	75.4	88.8	82.8
LLaVA-1.5-7B [34]	7.06	88.0	81.6	76.1	60.9	58.8	67.0	62.4
E5-V (LLaVA-Next-8B) [23]	8.36	96.7	89.5	85.3	75.0	70.1	89.2	83.5
E5-V (LLaVA-1.5-7B) [23]	7.06	95.8	86.6	81.6	62.9	64.0	93.5	88.0
VladVA (Ours) (LLaVA-1.5-7B)	7.06	**98.1**	**92.1**	**86.8**	**79.0**	**82.9**	**95.2**	**95.8**

4.1. Zero-shot image-text retrieval

We test our approach on the standard Flickr30k [46], MS-COCO [33] and nocaps [2] datasets, containing 1,000, 5,000 and 15,100 test samples respectively. For the latter, we simply average the results on the three partitions.

Across all three datasets, our approach significantly surpasses the current state-of-the-art models, including models of similar size. It even outperforms the much bigger EVA-CLIP (18B) model (85.0% vs. 83.3%) on Flickr30k, (59.0% vs. 55.6%) on MS-COCO and (72.3% vs. 69.3%) on nocaps in terms of @R1 for image retrieval. Similarly, we also outperform the LVLM-based E5-V model by 5.5% on Flickr30k, 6% on MS-COCO, and 6.2% on nocaps.

4.2. Image-text compositionality

Compositionality benchmarks construct hard negatives that elicit various types of compositional failures. Herein, we focus our comparison on the currently most challenging test sets, SugarCrepe [19] and SugarCrepe++ [16] (For Winoground [41] please see supp. material). For SugarCrepe++, we are primarily interested in the Image-to-Text (ITT) setting since the Text-to-Text (TOT) setting evaluates the language component of the methods only.

As Tables 2 and 3 show, our approach is the best in both SugarCrepe and SugarCrepe++ (ITT). On SugarCrepe, we outperform the 18B EVA-CLIP model on all categories, with particularly large gains on relation replacement (76.1 vs. 86.8), attribution adding (85.0 vs. 95.8), and object swapping (65.3 vs. 85.8). The last case is particularly interesting as it directly measures the *bag-of-words* behavior, showcasing the significant improvements our method achieves in this direction. Additionally, we outperform the E5-V variant based on the same LLaVA-1.5-7B model that we used, and the one based on the heavier LLaVA-Next-8B. A similar trend is observed on SugarCreppe++ where we outperform EVA-CLIP (18B) by up to 10.9% (on object swapping) and E5-V (ITT) in all but relation replacement. Note that, thanks to its text-text training, E5-V surpasses our method for the TOT setting, but we note that their loss can be readily incorporated into our framework, leaving this for future work.

5. Ablation studies

5.1. Impact of method's components

We quantify the impact of the proposed method's components by training on a smaller 1M subset, reporting results on SugarCrepe and on Flickr30k.

Impact of adaptation components: We start by measuring the impact of the efficient adaptation strategy based on soft prompting and adapter-finetuning. For simplicity, we ablate this by training using only the contrastive loss. As the results from Tab. 4 show, both components, individually and jointly, provide notable gains on top of the original LLaVA-1.5-7B model (i.e. the case of no adaptation).

While LoRA fine-tuning performs better than soft-prompting (due to its bigger capacity), the latter alone performs surprisingly well. To understand why, we analyze the changes the soft prompts undergo by finding the closest embedding in the LLM's vocabulary. This results in the following decoded sentences: "</s> '<Summarize the provided image in one word:/ $[" and, " ωaSummarize the provided text in one word:−". The two sentences remain unchanged semantically, with the only characters changed being the ones at the start and end of the prompt. Intuitively, this allows the

Table 3. Comparison with state-of-the-art on the SugarCrepe++ compositionality benchmark.

Method	Params	Swap Object		Swap Attribute		Replace Object		Replace Attribute		Replace Relation	
	(B)	ITT	TOT	ITT	TOT	ITT	TOT	ITT	TOT	ITT	TOT
Human	–	100.00	96.7	96.7	93.3	100.00	97.00	100.00	98.3	100.00	96.7
CLIP (ViT-B) [36]	0.15	45.2	19.7	45.2	33.0	86.8	83.7	65.6	59.1	56.3	38.62
CLIP (ViT-L) [36]	0.43	46.0	14.5	44.5	28.7	92.0	81.3	68.8	56.3	53.4	39.1
BLIP (ViT-L) [28]	0.23	46.8	29.8	60.1	52.5	92.6	89.1	71.7	75.0	56.8	57.7
BLIP2 (ViT-L) [29]	1.17	37.9	39.5	51.9	55.4	94.8	96.9	73.2	86.5	65.1	69.6
OpenCLIP (ViT-G/14) [37]	1.37	40.7	27.4	54.2	49.6	93.1	89.4	72.5	73.1	57.6	51.4
OpenCLIP (ViT-BigG/14) [37]	2.54	48.8	28.2	57.7	52.4	94.2	90.5	76.4	72.6	59.4	53.6
EVA-02-CLIP (ViT-E/14+) [38]	5.04	48.4	28.2	56.3	49.4	94.5	88.9	76.3	70.6	59.4	49.4
EVA-CLIP (8B) [39]	8.22	43.6	25.4	55.2	46.9	93.7	85.8	73.4	67.9	59.7	49.2
EVA-CLIP (18B) [39]	18.3	45.2	25.4	55.5	47.6	94.1	85.1	77.0	69.8	60.4	47.8
NegCLIP [47]	0.15	55.3	34.7	58.0	56.5	89.5	94.5	69.4	76.3	52.3	51.6
CLIP-SVLC [14]	0.15	43.0	18.9	48.4	34.6	80.9	91.6	57.0	66.9	47.3	51.3
BLIP-SGVL [18]	0.15	13.2	–	38.8	–	53.8	–	34.4	–	30.7	–
LLaVA-1.5-7B [34]	7.06	23.8	30.7	28.0	29.5	58.1	63.0	46.8	58.1	52.3	63.4
E5-V (LLaVA-Next-8B) [23]	8.36	50.8	**48.4**	49.7	56.9	93.1	**97.6**	76.1	**87.1**	**74.7**	**84.4**
E5-V (LLaVA-1.5-7B) [23]	7.06	39.5	42.3	40.7	48.5	89.7	94.6	71.7	86.4	72.0	81.5
VladVA (Ours) (LLaVA-1.5-7B)	7.06	**56.1**	36.7	**63.0**	**62.5**	**95.0**	93.0	**78.2**	82.3	71.1	66.3

Table 4. Impact of adaptation components and AR loss. All models are trained on 1M samples.

Method	AR	SugarCrepe			Flickr30k	
	loss	Replace	Swap	Add	T2I	I2T
LLaVA-1.5-7B	✗	81.9	59.8	64.7	59.6	65.6
+ soft-prom.	✗	86.4	66.9	89.3	76.7	91.7
+ adapter-ft.	✗	87.0	69.8	88.8	79.1	91.4
+ adapter-ft. + soft-prom.	✗	87.1	72.0	88.6	79.6	**92.9**
+ adapter-ft. + soft-prom.	✓	**89.5**	**75.5**	**89.5**	**80.6**	91.8

model to mark/specialize the token that should gather the visual or textual evidence for discriminative tasks.

Impact of AR loss: We measure the impact of the proposed autoregressive loss on long captions from Sec. 3.2.2. As Tab. 4 shows, the AR loss adds a notable performance boost across all datasets tested. Finally, we note that using the long captions in isolation, without the proposed training strategy and loss, does not result in measurable gains.

6. Conclusions

We introduced a new framework for adapting a *generative* LVLM into a *discriminative* model, unlocking its innate capability for powerful image-text discrimination and enhanced language understanding. Our framework uses both short and long captions for training the LVLM with contrastive and next-token prediction losses respectively. We also presented a parameter-efficient adaptation method using a combination of soft prompting and LoRA adapters. Finally, we showed that our approach results in significant improvements over state-of-the-art models of similar size for image-text retrieval and compositionality benchmarks.

7. Results for additional model sizes and architectures

To further showcase the generalizability of our approach, herein we report results on two additional models: LLaVA-1.5-13B [34] and Qwen2-VL-2B [43]. The 1st is a scaled-up version of the LLaVA-1.5-7B [34] used in the main manuscript and tests the scalability of our approach with size. The second follows a different architecture and training procedure and has "only" 2B parameters, testing both generalizations to different architectures and finetuning in a lower-parameters regime. As the results from Tables 5, 6 7 and 8 show, on all 6 datasets (*i.e*. Flickr, coco, nocaps, SugarCrepe, SugarCrepe++ and Winoground) for both retrieval and compositionality, in all cases we significantly improve upon the original zero-shot model performance, showing good scalability with size in both directions, *i.e*. for smaller and bigger models.

8. Compositionality evaluation on Winoground

In addition to the results from the main paper, herein, we report results on Winoground [41], a curated dataset consisting of 400 images with difficult/unusual scenarios that go beyond compositionality and largely act as a natural adversarial set [13, 47]. As the results from Table 8 show, our approach matches and outperforms prior models, including the large 18B EVA-CLIP model (17.5 vs. 15.0, 40.5 vs. 35.8 and 12.8 vs. 10.5, for image, text and respectively group set).

9. Zero-shot image recognition on ImageNet

From an evaluation point of view, the main focus of this work is on improved zero-shot retrieval and, more generally, improved vision-language compositional ability. We focus on these tasks, as they require stronger (vision-)language understanding abilities, which we show an LVLM can offer under appropriate training regimes. As a study case, herein, for completeness, we also measure the zero-shot ability of the model for image recognition on ImageNet [12]. As the results from Table 9 show, our approach significantly improves upon the zero-shot LVLM we start from (54.7 vs 70.6%). In comparison, E5-V approach only offers modest performance gains (45.8 vs 48.2%) and has notably lower performance than our approach (48.2 vs 70.6%) despite using a bigger model. While significantly improving upon the model we start from, the low data regime we train our model in (only 8.1M samples) limits its overall performance, with contrastive models trained on billion samples performing better. This is expected as the image recognition ability of a model, especially on the highly specific categories of ImageNet, will depend on how often (if at all) they are seen in the training set. This is especially significant given that many of the datasets used for contrastive learning are filtered based on the ImageNet classes [36]. In lower data regimes, comparable with ours, we can observe that our approach produces notably better results (*e.g.* 51.1% for FFF [7], trained on 15M samples vs 70.6% for ours). Finally, when comparing it with other models focusing on retrieval (*i.e.* BLIP and BLIP2) our approach outperforms either of them by more than 15% in absolute terms despite the fact that these models were trained on 129M samples. All in all, we outperform all models trained in comparable settings, showing promising initial results in this direction too.

Table 5. Zero-shot text-image retrieval accuracy on Flickr30K, COCO and nocaps.

Method	**image** retrieval						**text** retrieval					
	Flickr30K		COCO		nocaps		Flickr30K		COCO		nocaps	
	R@1	R@10	R@1	R@10	R@1	R@10	R@1	R@10	R@1	R@10	R@1	R@10
Qwen2-VL-2B [43]	54.1	86.0	32.4	68.2	41.2	80.1	59.6	89.2	35.3	71.8	54.0	90.3
VladVA (Ours) (`Qwen2-VL-2B`)	**80.4**	**97.3**	**52.5**	**84.4**	**68.3**	**94.9**	**93.7**	**99.9**	**71.9**	**93.9**	**86.0**	**99.4**
LLaVA-1.5-7B [34]	59.6	89.3	34.4	69.6	46.9	83.3	65.6	92.3	35.6	70.5	52.1	88.1
VladVA (Ours) (`LLaVA-1.5-7B`)	**85.0**	**98.5**	**59.0**	**88.6**	**72.3**	**96.5**	**94.3**	**99.9**	**72.9**	**94.4**	**85.7**	**99.5**
LLaVA-1.5-13B [34]	61.7	90.4	37.9	74.1	48.4	85.0	66.9	93.6	35.3	71.0	48.0	87.9
VladVA (Ours) (`LLaVA-1.5-13B`)	**85.6**	**98.6**	**58.2**	**88.4**	**74.0**	**96.6**	**94.5**	**99.8**	**75.0**	**95.6**	**85.4**	**99.6**

Table 6. Zero-shot results on SugarCrepe compositionality benchmark.

Method	Params	Replace			Swap		Add	
	(B)	Object	Attribute	Relation	Object	Attribute	Object	Attribute
Qwen2-VL-2B [43]	2.21	89.9	72.0	75.0	56.1	56.1	73.2	70.1
VladVA (Ours) (`Qwen2-VL-2B`)	2.21	**97.9**	**89.7**	**81.5**	**76.5**	**82.6**	**93.6**	**95.4**
LLaVA-1.5-7B [34]	7.06	88.0	81.6	76.1	60.9	58.8	67.0	62.4
VladVA (Ours) (`LLaVA-1.5-7B`)	7.06	**98.1**	**92.1**	**86.8**	**79.0**	**82.9**	**95.2**	**95.8**
LLaVA-1.5-13B [34]	13.35	90.0	80.6	76.3	71.8	61.9	69.3	59.1
VladVA (Ours) (`LLaVA-1.5-13B`)	13.35	**98.1**	**93.9**	**89.8**	**81.1**	**86.0**	**95.2**	**97.0**

Table 7. Zero-shot results on the SugarCrepe++ compositionality benchmark.

Method	Params	Swap Object		Swap Attribute		Replace Object		Replace Attribute		Replace Relation	
	(B)	ITT	TOT	ITT	TOT	ITT	TOT	ITT	TOT	ITT	TOT
Qwen2-VL-2B [43]	2.21	32.7	27.8	30.5	25.3	73.6	65.9	46.8	43.0	57.6	**58.3**
VladVA (Ours) (`Qwen2-VL-2B`)	2.21	**50.8**	**33.5**	**60.4**	**48.2**	**93.7**	**93.8**	**74.8**	**77.5**	**63.6**	57.4
LLaVA-1.5-7B [34]	7.06	23.8	30.7	28.0	29.5	58.1	63.0	46.8	58.1	52.3	63.4
VladVA (Ours) (`LLaVA-1.5-7B`)	7.06	**56.1**	36.7	**63.0**	**62.5**	**95.0**	93.0	**78.2**	82.3	71.1	66.3
LLaVA-1.5-13B [34]	13.35	35.5	32.3	30.2	32.4	68.7	66.8	44.8	43.1	52.3	55.6
VladVA (Ours) (`LLaVA-1.5-13B`)	13.35	**55.2**	**38.3**	**65.6**	**60.6**	**94.5**	**92.5**	**80.7**	**81.1**	**73.2**	**66.4**

Table 8. Comparison with state-of-the-art on the Winoground compositionality benchmark.

Model	Image	Text	Group
CLIP (ViT-B) [36]	10.5	25.0	7.3
CLIP (ViT-L) [36]	12.3	27.5	8.3
BLIP (ViT-L) [28]	10.0	30.5	7.8
BLIP2 (ViT-L) [29]	10.5	29.5	8.5
OpenCLIP (ViT-G/14) [37]	12.8	32.0	9.3
OpenCLIP (ViT-BigG/14) [37]	15.5	35.5	12.0
EVA-02-CLIP (ViT-E/14+) [38]	14.0	33.8	10.8
EVA-CLIP (8B) [39]	14.8	36.5	10.3
EVA-CLIP (18B) [39]	15.0	35.8	10.5
NegCLIP [47]	10.5	29.5	8.0
LLaVA-1.5-7B [34]	11.3	18.5	6.5
E5-V (LLaVA-Next-8B) [23]	14.8	32.3	11.3
E5-V (LLaVA-1.5-7B) [23]	17.4	31.3	10.5
VladVA (Ours) (LLaVA-1.5-7B)	**17.5**	**40.5**	**12.8**

Table 9. Zero-shot image recognition results on ImageNet dataset in terms of Top-1 and Top-5 (%) accuracy.

Model	Data. size	Top-1	Top-5
CLIP (ViT-B) [36]	400M	68.4	91.9
CLIP (ViT-L) [36]	400M	74.0	94.0
EVA-CLIP (18B) [39]	2.7B	83.5	97.2
CLIP (ViT-B) [36]	15M	32.8	-
HiDeCLIP (ViT-B) [36]	15M	45.9	-
FFF (ViT-B) [7]	15M	51.1	-
BLIP (ViT-L) [28]	129M	54.2	81.5
BLIP2 (ViT-L) [29]	129M	46.7	74.2
LLaVA-Next-8B [26]	0M	45.8	74.6
E5-V [23] (LLaVA-Next-8B)	0M	48.2	76.6
LLaVA-1.5-7B [34]	0M	42.0	74.6
VladVA (Ours) (LLaVA-1.5-7B)	8.1M	63.7	88.3
Qwen2-VL-2B [43]	0M	54.7	79.4
VladVA (Ours) (Qwen2-VL-2B)	8.1M	70.6	91.1

10. Qualitative text generation examples post discriminative adaptation

Our main objective is to convert generative LVLMs into discriminative ones, hence the proposed approach is designed from the perspective of maximizing the discriminative abilities of the model. Still, it may be interesting to qualitatively see how our model, and the closest relevant approach E5-V behave. We note, that in principle both our approach and E5-V use LoRAs adapters, hence it is easy to switch between the discriminative and the generative mode without compromising either, by enabling or disabling the adapters. That being said, herein we present some qualitative examples post-training, so we can see the direct effect the training has on the model. As the results from Fig.7 show, generally, our approach better retains the generative capabilities of the model post-training, producing fine-grained captions, similar with the original ones. In contrast, E5-V appears to predominantly produce only very-shot, not-descriptive outputs.

Prompt: Give a detailed description of the image.

LLaVA-1.5-7B:

The image depicts a busy city street filled with people walking and standing around. There are numerous individuals scattered throughout the scene, some walking in groups and others walking alone. A few people are carrying handbags, and a couple of umbrellas can be seen in the crowd.

The street is lined with various shops, including a bicycle shop, which is located on the right side of the street. A clock is also visible in the scene, hanging above the street, likely indicating the time for passersby. The overall atmosphere of the image is bustling and lively, with people going about their daily activities.

E5-V (LLaVA-1.5-7B):

People are crossing the street at a crosswalk.

Ours (LLaVA-1.5-7B):

This is a bustling street scene in Japan, teeming with life and activity. The street is lined with a variety of shops and stalls, each with its own unique offerings. The shops are housed in buildings painted in vibrant hues of red, yellow, and blue, adding a splash of color to the scene. The shops are adorned with signs written in Japanese, indicating a local market or shopping area. The street itself is a hive of activity, with people walking around, some carrying bags, possibly returning from a shopping spree. The street is also marked with traffic lights and street signs, ensuring order amidst the hustle and bustle. The image captures the essence of a typical day in a busy Japanese shopping district, filled with color, activity, and local charm.

Prompt: Describe the image briefly.

LLaVA-1.5-7B:

A small dog is wearing a pink and white costume, which includes a hood and a carrot. The dog is standing on a pink carpet, and it appears to be smiling. The dog is positioned in the center of the image, and the carpet extends to the edges of the frame.

E5-V (LLaVA-1.5-7B):

Poodle wearing a costume.

Ours (LLaVA-1.5-7B):

A small dog, wearing a pink pig costume, is sitting on a pink floor. The costume is complete with a hood and a carrot in its mouth. The dog's tongue is sticking out, adding a playful touch to the scene. The costume is detailed with a pink nose and ears, and a pink bow on the chest. The dog is sitting in front of a pink wall, which features a pink castle design. The overall image is a charming and adorable representation of a pet in a costume.

Prompt: Describe the image very briefly.

LLaVA-1.5-7B:

A man is walking down a street in front of a store with a large potted plant hanging from a pole. The store is called De Neude.

E5-V (LLaVA-1.5-7B):

Potted plant in a pot on a pole.

Ours (LLaVA-1.5-7B):

A man is walking past a storefront with a large flower pot hanging from the ceiling. The storefront is green and white, and there's a sign that reads "De Neude". The man is wearing a red shirt and is walking past a bicycle. The street is lined with buildings and there are several signs and advertisements. The overall atmosphere suggests a busy city street.

Prompt: Provide a conscise description of this image.

LLaVA-1.5-7B:

A black car is driving down a street in front of a stop sign. The car is passing by a red and white building with a Chinese design. There are several people walking on the sidewalk, and a few of them are carrying handbags. The scene also includes a fire hydrant and a potted plant.

E5-V (LLaVA-1.5-7B):

stop sign on a pole.

Ours (LLaVA-1.5-7B):

A red stop sign is in front of a red and gold archway. The archway is adorned with Chinese characters and has a lion statue guarding it. A black car is driving by the archway.

Figure 7. **Qualitative comparison on image captioning** of the base LLaVA-1.5-7B model and its fine-tuned versions using both E5-V [23] and our proposed method. We show that with our method, the LLaVA-1.5-7B better retains its captioning capabilities, while E5-V fine-tuning appears to result in less informative captions.

References

[1] Marah Abdin, Sam Ade Jacobs, Ammar Ahmad Awan, Jyoti Aneja, Ahmed Awadallah, Hany Awadalla, Nguyen Bach, Amit Bahree, Arash Bakhtiari, Harkirat Behl, et al. Phi-3 technical report: A highly capable language model locally on your phone. *arXiv preprint arXiv:2404.14219*, 2024. 2

[2] Harsh Agrawal, Karan Desai, Yufei Wang, Xinlei Chen, Rishabh Jain, Mark Johnson, Dhruv Batra, Devi Parikh, Stefan Lee, and Peter Anderson. Nocaps: Novel object captioning at scale. In *Proceedings of the IEEE/CVF international conference on computer vision*, pages 8948–8957, 2019. 7

[3] Jinze Bai, Shuai Bai, Shusheng Yang, Shijie Wang, Sinan Tan, Peng Wang, Junyang Lin, Chang Zhou, and Jingren Zhou. Qwen-vl: A frontier large vision-language model with versatile abilities. *arXiv preprint arXiv:2308.12966*, 2023. 2

[4] Yonatan Bitton, Hritik Bansal, Jack Hessel, Rulin Shao, Wanrong Zhu, Anas Awadalla, Josh Gardner, Rohan Taori, and Ludwig Schmidt. Visit-bench: A benchmark for vision-language instruction following inspired by real-world use. *arXiv preprint arXiv:2308.06595*, 2023. 2

[5] Tom B Brown. Language models are few-shot learners. *arXiv preprint arXiv:2005.14165*, 2020. 1, 2

[6] Adrian Bulat and Georgios Tzimiropoulos. LASP: Text-to-text optimization for language-aware soft prompting of vision & language models. In *Proceedings of the IEEE/CVF Conference on Computer Vision and Pattern Recognition*, pages 23232–23241, 2023. 5

[7] Adrian Bulat, Yassine Ouali, and Georgios Tzimiropoulos. FFF: Fixing flawed foundations in contrastive pre-training results in very strong vision-language models. In *Proceedings of the IEEE/CVF Conference on Computer Vision and Pattern Recognition*, pages 14172–14182, 2024. 2, 9, 10

[8] Lin Chen, Jinsong Li, Xiaoyi Dong, Pan Zhang, Conghui He, Jiaqi Wang, Feng Zhao, and Dahua Lin. Sharegpt4v: Improving large multi-modal models with better captions. *arXiv preprint arXiv:2311.12793*, 2023. 4

[9] Yangyi Chen, Karan Sikka, Michael Cogswell, Heng Ji, and Ajay Divakaran. Measuring and improving chain-of-thought reasoning in vision-language models. *arXiv preprint arXiv:2309.04461*, 2023. 1

[10] Xiangxiang Chu, Limeng Qiao, Xinyu Zhang, Shuang Xu, Fei Wei, Yang Yang, Xiaofei Sun, Yiming Hu, Xinyang Lin, Bo Zhang, et al. Mobilevlm v2: Faster and stronger baseline for vision language model. *arXiv preprint arXiv:2402.03766*, 2024. 2

[11] Matt Deitke, Christopher Clark, Sangho Lee, Rohun Tripathi, Yue Yang, Jae Sung Park, Mohammadreza Salehi, Niklas Muennighoff, Kyle Lo, Luca Soldaini, et al. Molmo and pixmo: Open weights and open data for state-of-the-art multimodal models. *arXiv preprint arXiv:2409.17146*, 2024. 1, 2

[12] Jia Deng, Wei Dong, Richard Socher, Li-Jia Li, Kai Li, and Li Fei-Fei. Imagenet: A large-scale hierarchical image database. In *2009 IEEE conference on computer vision and pattern recognition*, pages 248–255. Ieee, 2009. 9

[13] Anuj Diwan, Layne Berry, Eunsol Choi, David Harwath, and Kyle Mahowald. Why is winoground hard? investigating failures in visuolinguistic compositionality. *arXiv preprint arXiv:2211.00768*, 2022. 8

[14] Sivan Doveh, Assaf Arbelle, Sivan Harary, Eli Schwartz, Roei Herzig, Raja Giryes, Rogerio Feris, Rameswar Panda, Shimon Ullman, and Leonid Karlinsky. Teaching structured vision & language concepts to vision & language models. In *Proceedings of the IEEE/CVF Conference on Computer Vision and Pattern Recognition*, pages 2657–2668, 2023. 8

[15] Abhimanyu Dubey, Abhinav Jauhri, Abhinav Pandey, Abhishek Kadian, Ahmad Al-Dahle, Aiesha Letman, Akhil Mathur, Alan Schelten, Amy Yang, Angela Fan, et al. The llama 3 herd of models. *arXiv preprint arXiv:2407.21783*, 2024. 1

[16] Sri Harsha Dumpala, Aman Jaiswal, Chandramouli Sastry, Evangelos Milios, Sageev Oore, and Hassan Sajjad. Sugarcrepe++ dataset: Vision-language model sensitivity to semantic and lexical alterations. *arXiv preprint arXiv:2406.11171*, 2024. 7

[17] Gabriel Goh, Nick Cammarata, Chelsea Voss, Shan Carter, Michael Petrov, Ludwig Schubert, Alec Radford, and Chris Olah. Multimodal neurons in artificial neural networks. *Distill*, 6(3):e30, 2021. 2

[18] Roei Herzig, Alon Mendelson, Leonid Karlinsky, Assaf Arbelle, Rogerio Feris, Trevor Darrell, and Amir Globerson. Incorporating structured representations into pretrained vision & language models using scene graphs. *arXiv preprint arXiv:2305.06343*, 2023. 8

[19] Cheng-Yu Hsieh, Jieyu Zhang, Zixian Ma, Aniruddha Kembhavi, and Ranjay Krishna. Sugarcrepe: Fixing hackable benchmarks for vision-language compositionality. *Advances in neural information processing systems*, 36, 2024. 1, 2, 7

[20] Edward J Hu, Yelong Shen, Phillip Wallis, Zeyuan Allen-Zhu, Yuanzhi Li, Shean Wang, Lu Wang, and Weizhu Chen. Lora: Low-rank adaptation of large language models. *arXiv preprint arXiv:2106.09685*, 2021. 2, 5

[21] Chao Jia, Yinfei Yang, Ye Xia, Yi-Ting Chen, Zarana Parekh, Hieu Pham, Quoc Le, Yun-Hsuan Sung, Zhen Li, and Tom Duerig. Scaling up visual and vision-language representation learning with noisy text supervision. In *International conference on machine learning*, pages 4904–4916. PMLR, 2021. 1

[22] Albert Q Jiang, Alexandre Sablayrolles, Arthur Mensch, Chris Bamford, Devendra Singh Chaplot, Diego de las Casas, Florian Bressand, Gianna Lengyel, Guillaume Lample, Lucile Saulnier, et al. Mistral 7b. *arXiv preprint arXiv:2310.06825*, 2023. 2

[23] Ting Jiang, Minghui Song, Zihan Zhang, Haizhen Huang, Weiwei Deng, Feng Sun, Qi Zhang, Deqing Wang, and Fuzhen Zhuang. E5-v: Universal embeddings with multimodal large language models. *arXiv preprint arXiv:2407.12580*, 2024. 1, 2, 4, 6, 7, 8, 10, 11

[24] Chankyu Lee, Rajarshi Roy, Mengyao Xu, Jonathan Raiman, Mohammad Shoeybi, Bryan Catanzaro, and Wei Ping. Nv-embed: Improved techniques for training llms as generalist embedding models. *arXiv preprint arXiv:2405.17428*, 2024. 2

[25] Martha Lewis, Nihal V Nayak, Peilin Yu, Qinan Yu, Jack Merullo, Stephen H Bach, and Ellie Pavlick. Does clip bind

concepts? probing compositionality in large image models. *arXiv preprint arXiv:2212.10537*, 2022. 1, 2

[26] Bo Li, Kaichen Zhang, Hao Zhang, Dong Guo, Renrui Zhang, Feng Li, Yuanhan Zhang, Ziwei Liu, and Chunyuan Li. Llava-next: Stronger llms supercharge multimodal capabilities in the wild, 2024. 1, 2, 10

[27] Feng Li, Renrui Zhang, Hao Zhang, Yuanhan Zhang, Bo Li, Wei Li, Zejun Ma, and Chunyuan Li. Llava-next-interleave: Tackling multi-image, video, and 3d in large multimodal models. *arXiv preprint arXiv:2407.07895*, 2024. 1, 2

[28] Junnan Li, Dongxu Li, Caiming Xiong, and Steven Hoi. Blip: Bootstrapping language-image pre-training for unified vision-language understanding and generation. In *International conference on machine learning*, pages 12888–12900. PMLR, 2022. 1, 6, 7, 8, 10

[29] Junnan Li, Dongxu Li, Silvio Savarese, and Steven Hoi. Blip-2: Bootstrapping language-image pre-training with frozen image encoders and large language models. In *International conference on machine learning*, pages 19730–19742. PMLR, 2023. 2, 4, 6, 7, 8, 10

[30] Xiang Lisa Li and Percy Liang. Prefix-tuning: Optimizing continuous prompts for generation. *arXiv preprint arXiv:2101.00190*, 2021. 2, 5

[31] Yangguang Li, Feng Liang, Lichen Zhao, Yufeng Cui, Wanli Ouyang, Jing Shao, Fengwei Yu, and Junjie Yan. Supervision exists everywhere: A data efficient contrastive language-image pre-training paradigm. *arXiv preprint arXiv:2110.05208*, 2021. 1

[32] Yanwei Li, Yuechen Zhang, Chengyao Wang, Zhisheng Zhong, Yixin Chen, Ruihang Chu, Shaoteng Liu, and Jiaya Jia. Mini-gemini: Mining the potential of multi-modality vision language models. *arXiv preprint arXiv:2403.18814*, 2024. 2

[33] Tsung-Yi Lin, Michael Maire, Serge Belongie, James Hays, Pietro Perona, Deva Ramanan, Piotr Dollár, and C Lawrence Zitnick. Microsoft coco: Common objects in context. In *Computer Vision–ECCV 2014: 13th European Conference, Zurich, Switzerland, September 6-12, 2014, Proceedings, Part V 13*, pages 740–755. Springer, 2014. 1, 7

[34] Haotian Liu, Chunyuan Li, Yuheng Li, and Yong Jae Lee. Improved baselines with visual instruction tuning. In *Proceedings of the IEEE/CVF Conference on Computer Vision and Pattern Recognition*, pages 26296–26306, 2024. 2, 6, 7, 8, 9, 10

[35] Haotian Liu, Chunyuan Li, Qingyang Wu, and Yong Jae Lee. Visual instruction tuning. *Advances in neural information processing systems*, 36, 2024. 2

[36] Alec Radford, Jong Wook Kim, Chris Hallacy, Aditya Ramesh, Gabriel Goh, Sandhini Agarwal, Girish Sastry, Amanda Askell, Pamela Mishkin, Jack Clark, et al. Learning transferable visual models from natural language supervision. In *International conference on machine learning*, pages 8748–8763. PMLR, 2021. 1, 2, 6, 7, 8, 9, 10

[37] Christoph Schuhmann, Romain Beaumont, Richard Vencu, Cade Gordon, Ross Wightman, Mehdi Cherti, Theo Coombes, Aarush Katta, Clayton Mullis, Mitchell Wortsman, et al. Laion-5b: An open large-scale dataset for training next generation image-text models. *Advances in Neural Information Processing Systems*, 35:25278–25294, 2022. 2, 6, 7, 8, 10

[38] Quan Sun, Yuxin Fang, Ledell Wu, Xinlong Wang, and Yue Cao. Eva-clip: Improved training techniques for clip at scale. *arXiv preprint arXiv:2303.15389*, 2023. 6, 7, 8, 10

[39] Quan Sun, Jinsheng Wang, Qiying Yu, Yufeng Cui, Fan Zhang, Xiaosong Zhang, and Xinlong Wang. Eva-clip-18b: Scaling clip to 18 billion parameters. *arXiv preprint arXiv:2402.04252*, 2024. 6, 7, 8, 10

[40] Gemma Team, Thomas Mesnard, Cassidy Hardin, Robert Dadashi, Surya Bhupatiraju, Shreya Pathak, Laurent Sifre, Morgane Rivière, Mihir Sanjay Kale, Juliette Love, et al. Gemma: Open models based on gemini research and technology. *arXiv preprint arXiv:2403.08295*, 2024. 2

[41] Tristan Thrush, Ryan Jiang, Max Bartolo, Amanpreet Singh, Adina Williams, Douwe Kiela, and Candace Ross. Winoground: Probing vision and language models for visio-linguistic compositionality. In *Proceedings of the IEEE/CVF Conference on Computer Vision and Pattern Recognition*, pages 5238–5248, 2022. 7, 8

[42] Hugo Touvron, Thibaut Lavril, Gautier Izacard, Xavier Martinet, Marie-Anne Lachaux, Timothée Lacroix, Baptiste Rozière, Naman Goyal, Eric Hambro, Faisal Azhar, et al. Llama: Open and efficient foundation language models. *arXiv preprint arXiv:2302.13971*, 2023. 1, 2

[43] Peng Wang, Shuai Bai, Sinan Tan, Shijie Wang, Zhihao Fan, Jinze Bai, Keqin Chen, Xuejing Liu, Jialin Wang, Wenbin Ge, et al. Qwen2-vl: Enhancing vision-language model's perception of the world at any resolution. *arXiv preprint arXiv:2409.12191*, 2024. 8, 9, 10

[44] Weihan Wang, Qingsong Lv, Wenmeng Yu, Wenyi Hong, Ji Qi, Yan Wang, Junhui Ji, Zhuoyi Yang, Lei Zhao, Xixuan Song, et al. Cogvlm: Visual expert for pretrained language models. *arXiv preprint arXiv:2311.03079*, 2023. 2

[45] Chenfei Wu, Shengming Yin, Weizhen Qi, Xiaodong Wang, Zecheng Tang, and Nan Duan. Visual chatgpt: Talking, drawing and editing with visual foundation models. *arXiv preprint arXiv:2303.04671*, 2023. 2

[46] Peter Young, Alice Lai, Micah Hodosh, and Julia Hockenmaier. From image descriptions to visual denotations: New similarity metrics for semantic inference over event descriptions. *Transactions of the Association for Computational Linguistics*, 2:67–78, 2014. 1, 3, 7

[47] Mert Yuksekgonul, Federico Bianchi, Pratyusha Kalluri, Dan Jurafsky, and James Zou. When and why vision-language models behave like bags-of-words, and what to do about it? *arXiv preprint arXiv:2210.01936*, 2022. 1, 2, 6, 7, 8, 10

[48] Xiaohua Zhai, Basil Mustafa, Alexander Kolesnikov, and Lucas Beyer. Sigmoid loss for language image pre-training. In *Proceedings of the IEEE/CVF International Conference on Computer Vision*, pages 11975–11986, 2023. 1, 2

[49] Kaiyang Zhou, Jingkang Yang, Chen Change Loy, and Ziwei Liu. Learning to prompt for vision-language models. *International Journal of Computer Vision*, 130(9):2337–2348, 2022. 5

[50] Deyao Zhu, Jun Chen, Xiaoqian Shen, Xiang Li, and Mohamed Elhoseiny. Minigpt-4: Enhancing vision-language understanding with advanced large language models. *arXiv preprint arXiv:2304.10592*, 2023. 1, 2